ISSN: 0067-2904

The Digital Change Detection for Low Resolution Satellite Images in Weathering Estimation

Alaa S. Mahdi
Remote Sensing Unit, College of Science, University of Baghdad, Baghdad, Iraq

Received: 15/2/2022 Accepted: 8/8/2022 Published: 28/2/2023

Abstract

The detection and estimation of weathering conditions have become a very important daily necessity in our life. For this purpose, several satellites of low resolution imagery were launched by the weathering and environmental agencies. The important weather paremeters are temperuter, wind direction, velocity, clould and humidity, etc. The low resolution images often deal with large-scale phenomena and the interpretation and projection of the produced data requires continuous development of tools and criteria.

In this paper, the low spatial resolution data generated by the moderate resolution imaging spectroradiometer (MODIS) were used to monitor the cloud density and direction above Iraq and its neighboring countries for the period from 14-12-2021 to 23-12-2021. The MODIS reflectance and surface temperature (HDF format) data were used and processed to achieve the purpose of this research. The reflectance data were projected according to a sinusoidal system due to the presence of three Earth zones distributions (37, 38, and 39, N). The cloud density was estimated from the digital values and the wind direction was estimated from the bands animation. The direction of wind for the cloudy condition was from the North-East. The digital data processing included data preparation and selection, georeference (adding a projection system), features extraction, and displaying the final results. All data were evaluated using ENVI (Environment for Visualizing Images, ver. 4.5.)

Keywords: low resolution image, weathering estimation, MODIS, Iraq, ENVI.

كشف التغاير الرقمي للصور الفضائية منخفضة الدقة التميزية في التوقعات الجوية

علاء سعود مهدي
وحدة الاستشعار عن بعد، كلية العلوم، جامعة بغداد، بغداد، العراق

الخلاصه

لقد أصبح توقع الحالة الجوية من الأمور اليومية المهمة في حياتنا. ولهذا الغرض أطلقت عدة سواتل فضائية منخفضة الدقة التميزية والتي تشغل وتدار من قبل وكالات خاصة. تتضمن العوامل الجوية، درجات الحرارة، اتجاه وسرعة الرياح، الغيوم والرطوبة النسبية، الخ. غالبا ما يستخدم لهذا الغرض

*Email: dralaa_smahdi@yahoo.com

المرئيات الفضائية منخفضة الدقة التميزية والتي ترصد ظاهرة طبيعية كبيرة، وتحتاج إلى أنظمة إسقاط خاصة، وبعض المعالجات الأخرى.

في هذا البحث تم استخدام بيانات المتحسس (MODIS) ذو الدقة التميزية الواطئة لغرض متابعة وتقدير كثافة الغيوم فوق العراق ودول الجوار للفترة من 12-14-2021 إلى 12-23-2021. لقد تم استخدام بيانات الانعكاسية، ودرجة حرارة السطح من نوع (HDF format data) لغرض تحقيق الغرض من البحث. تم تصحيح بيانات الانعكاسية وفقا للمسقط sinusoidal system وذلك بسبب وجود ثلاث انطقة لمنطقة الدراسة،(37، 38، و 39). إن كثافة الغيوم يمكن تحديدها من قيم الوحدات الصورية للبيانات بينما تم تحديد اتجاه الرياح من خلال عمل نموذج حي لعرض البيانات بصورة متتابعة. تضمن موضوع المعالجة الرقمية للبيانات، تهيئة واختيار البيانات، التصحيح الهندسي وإضافة المسقط، استخراج عناصر البيانات وعرض النتائج. تم العمل باستخدام البرنامج ENVI (Environment for Visualizing Images) الإصدار 4.5.

1. Introduction

The weather monitoring and estimation is considered as an important application of remotely sensed data which has a remarkable interest in humans daily life. For this purpose, several spaceborne and airborne sensors in different spectral bands were designed and launched, **[1]**. These sensors have low spatial resolution and utilized for monitoring and recording large areas or large-scale phenomena. Clouds are the major factor that controls water balance and energy in the Earth. Also, the cloud condition is characterized by often uncertain sources and components, [**1**]. A cloud can be defined, according to the American Meteorological Society's Glossary of Meteorology, as a visible aggregate of minute water droplets and/or ice particles in the atmosphere above the Earth's surface, [**2]**. The monitoring of cloud areas by satellite imagery involves many parameters and limitations. Clouds could be monitor through high reflectance in the visible band and low radiation emission in the thermal bands, **[2]**.

The Moderate Resolution Imaging Spectroradiometer data, (Reflectance and Surface temperature were used to detect and monitor the clouds over different regions of interest, **[3]**. The (MODIS) is a an instrument that was launched by the National Aeronautics and Space Administration (NASA) in 1999, the MODIS employs two satellites, (Terra satellite, 1999, Aqua satellite 2002). These satellites provide a global view for the Earth's surface and atmosphere in 36 different spectral bands. The MODIS spatial resolutions are 250 m, 500 m, and 1 km distributed through the spectral bands, The visible and reflected bands are those of 250 to 500 m, whereas, the thermal band are of 1 km in spatial resolutions, see appendix A. The spectral bands are variable from 8-bit to 16-bit images, [**3**]. The (NASA earthdata) website provides the user with many types of MODIS data which are coded in a particular format. Hence, the user must select the perfect type of MODIS data according to the research problem, size of region of interest, the nature of this region, for download request and data format details, visit the https://urs.earthdata.nasa.gov/home.

2. Region of Interest and Available Data

The region of interest is a full MODIS scene of an area of 1200*1200 km^2 which is assigned in the MODIS data index as "Coordinates**:** 35.0468 , 43.0305". The main scene area represent the Iraq country and a parts of all neighboring countries except. The geographic corners of the Region Of Interest, ROI can be given as;

NW corner, Lat. 40° 01′ 40.09″ N, Long. 39° 00′ 52.20″ E
NE corner, Lat. 39° 59′ 56.76″ N, Long. 52° 13′ 56.28″ E
SW corner, Lat. 29° 52′ 58.08″ N, Long. 34° 29′ 24″ E
SE corner, Lat. 29° 51′ 32.04″ N, Long. 46° 10′ 02.28″ E

The topography of the study area is vary from flat terrain to ragged terrain. The flatness goes to the south of the area, while the elevation from the sea level is about 1000 m in North to 7 meter in South. Two capital cites are found in the area, namely Baghdad and Amman, whereas many other big cities can also be found. The water resources can be found as a part of the Caspian sea, rivers, and lakes. The precipitation of this area is bout 100 mm in North to few millimeters in South. . The vegetation areas are concentrate in the northern part of the studied area and degraded toward the south; therefore, the south-western part of the area can be describe as desert. Figure 1 represents the ROI.

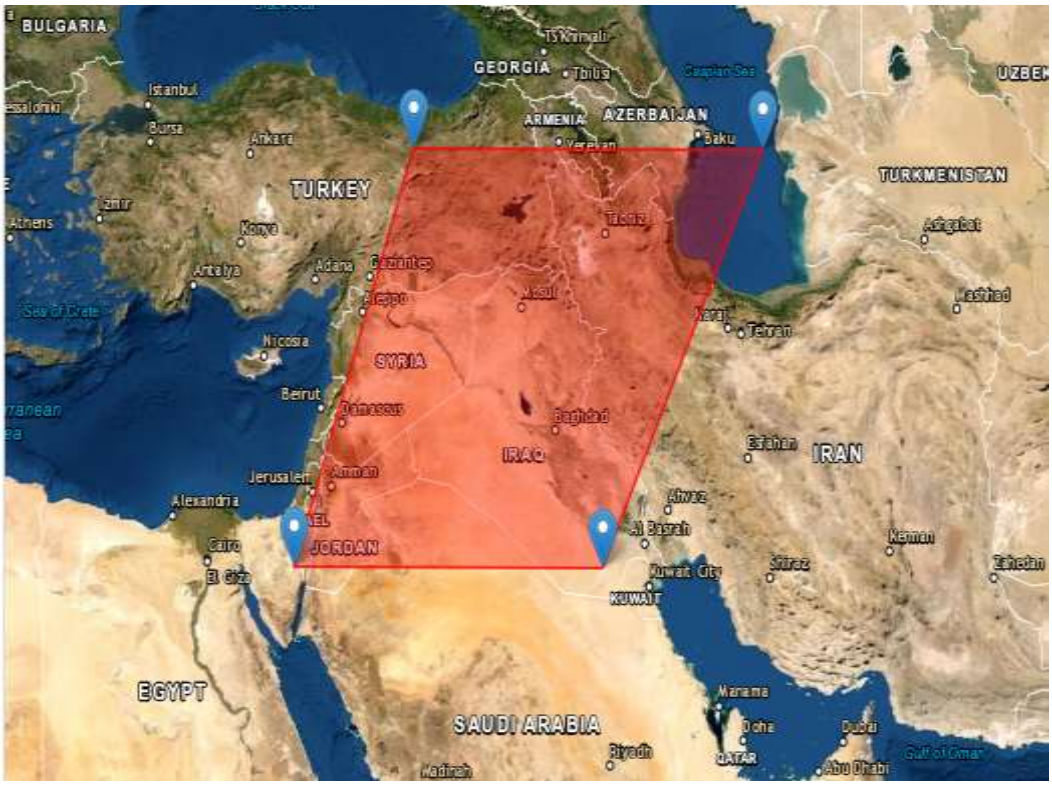

Figure 1: Location of The ROI, (Ref., USGS, Earth Explorer)

The available data are satellite imagery from the MODIS Terra and Aqua sensors for the reflectance and surface temperature bands. These data are free to downloaded from the USGS Earth Explorer and NASA Earthdata websites. The used data in this research are daily Level 2 MOD09GA, Terra/Aqua Surface Reflectance of 250 m, 500 m to 1 km spatial resolution, (from band 1 to band 7), and, the daily surface temperature Level 3 MOD11A1 (1) km in spatial resolution, (band 31 & band 32). This mode of data was georeferenced to sinusoidal projection, [**3**]. The data period is 10 days from 12/14/2021 to 12/23/2021, the reasons of selecting this time of the year are related to the cloud frequency increase and also temperature decrease. The temperature decrease is related with the using of MOD11A1 mode.

3. The Cloud Overview

The clouds are considered as important factor in all climatic and weather conditions. Also, many cloud caused a rain which is control the energy balance on the Earth. The monitoring of cloud by satellite data became more convenient in climatic and weather estimation, this remotely sensed application save time and public to all sites on the Earth. According to international cloud atlas, the clouds can be classified with respect to highest form the earth surface, such as, low cloud; (less than 2km), medium cloud; (2-7 km), high

cloud; (5-13 km). The highest of clouds is depends upon several factors, i.e. environmental and climatic factors, [**4**].

4. Research Methodology

The methodology of this research includes the data description and pre-processing, cloud extraction from the reflectance mode, digital change detection, comparing the reflectance results with the thermal bands, and cloud animation. The animation facility in the ENVI provides a display of the band in sequence that the images appears as movies.

4.1 Data Description and Pre-Processing

The NASA Earthdata provided several types of MODIS reflectance modes including different spatial, spectral, and temporal resolutions. The 8 day MODIS Terra/Aqua band 1-7, Surface Reflectance 8-Day L3 Global 500 m, MOD09A1, records the best observations in 8 day, i.e. the image is free from cloud, shadow and aerosol. This mode is not used in the current research due to cloud decline. The MOD09GA L2 daily MODIS band 1-7 surface reflectance at 500 m to 1 km resolution was used in cloud detection and monitoring. This type of data was provided with out projection reference and record all cloud, shadow, and aerosol, the band size is 2400*2400 for 500 m, and 1200*1200 for 1 km. The Land Surface Temperature, LST mode, daily collected, level 3 (band 31 & band 32) at 1km spatial resolution was projected to Sinusoidal projection. The band size is 1200 * 1200 within the area for each square km being about 0.928km by 0.928km, [**5**].

The re-processing of remotely sensed data before any calculation of image features is necessary to remove distortion and georeference the image data, [**6**]. The data set of MOD09GA was re-projected to sinusoidal projection using the ENVI correction facility. For this purpose, the reference MOD11A1 mode data were used to projected the input MOD09GA. By selection the upper left point coordinates values, the start pixels , and ground spatial resolution, such as, Projection; Sinusoidal, upper left point pixels (1,1) , ground coordinates (3335851.5593E, 4447802.0791N) m, Pixel size on the ground; 926.62543314 m. In the correction process the pixel size on the ground is was divide by 2 because the reference image is of 1 km.

At this point of view, the MOD09GA and MOD11A1 have the same projections, and areas, but in different spatial resolutions, figure 2 shows an example of MOD09GA & MOD11A1. Reflectance bands 1, 4, & 3 , 500 m Resolution Surface Temp. bands 31, & 23, 1km Resolution

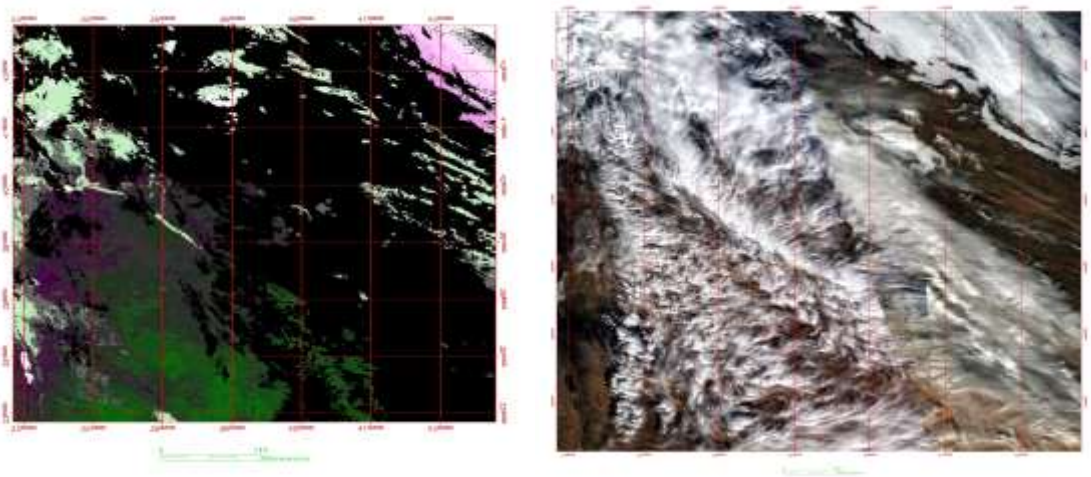

Figure 2: Examples of MOD09GA & MOD11A1 MODIS data, (date, 12/14/2021)

4.2 The Digital Cloud Extraction

A threshold value method was applied to extract the cloud pixel from each reflectance scene. The best reflectance bands for cloud detection are (b1; Red, b2; NIR, b3; Blue), [**7**]. The reflectance origin (Hierarchical Data Format), HDF spectral resolution is (8-16) bit. From the statistical analysis of the band the maximum pixel values is about 15300. This digit number represents the cloud pixels, because the cloud has high reflectance in the visible and NIR bands. The following expression was used in Band Math facility as, [**8**];

$$\text{Cloud pixel} = (b1 \text{ gt } 7000) * b1 \quad (1)$$

Where, b1 is any band in the reflectance mode.

7000, cloud detector threshold value. The (gt) term in equation 1 is to select the pixels values above 7000, and multiply them by the band values to avoid the result of binary image, i.e. the results hold the real cloud pixel values. Figure 3 illustrates an example of cloud extraction.

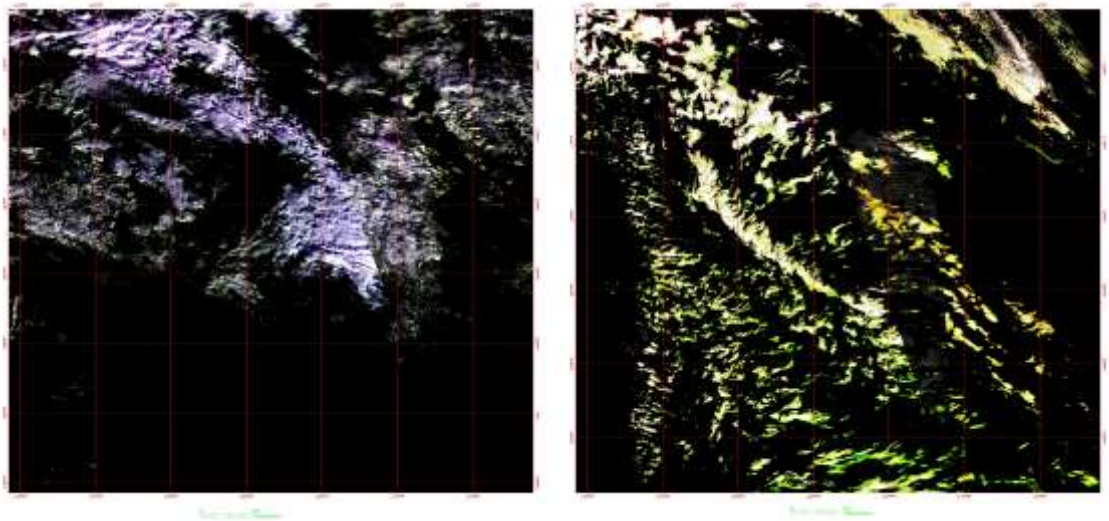

12/14/2021 12/23/2021

Figure 3: The Threshold Value Result Example

In figure 3, the change in cloud is illustrated visually, and the color difference between the two images refers to variations in cloud pixels values. Note that due to high image size the projection coordinates appear weakly.

4.3 The Digital Cloud Change Detection

At this point of view, the digital change will be calculated and extracted. The digital change detection techniques are well known. Many conditions must be available before any digital change detection process. These conditions includes, (1) same ground spatial resolutions, although from different sensors, (2) same spectral resolutions and bands, and (3) the images matching accuracy must be less than half pixel, [**9**]. The important factor at this stage is to decide to which bands must be used from the 10 days. The applied bands must be associated with the change methods. The famous change detection methods are, image differencing, rationing, and principal components analysis as change detector. For this case of data the differencing and rationing yields a long series of change images. Hence, the Principal Component Analysis (PCA) is the convenient method to extract the clod change during 10 days. In this method, the 1st bands from each cloud threshold images were merged in one file of 10 bands. The same way was applied for the 2nd bands and 3rd bands. After applying the Principal Component Analysis, PCA kernel, the PC1 represented no image change PC2 is image change, and the other PCs are noise. Figure 4 presents the change of cloud threshold by PCA kernel, **[10].**

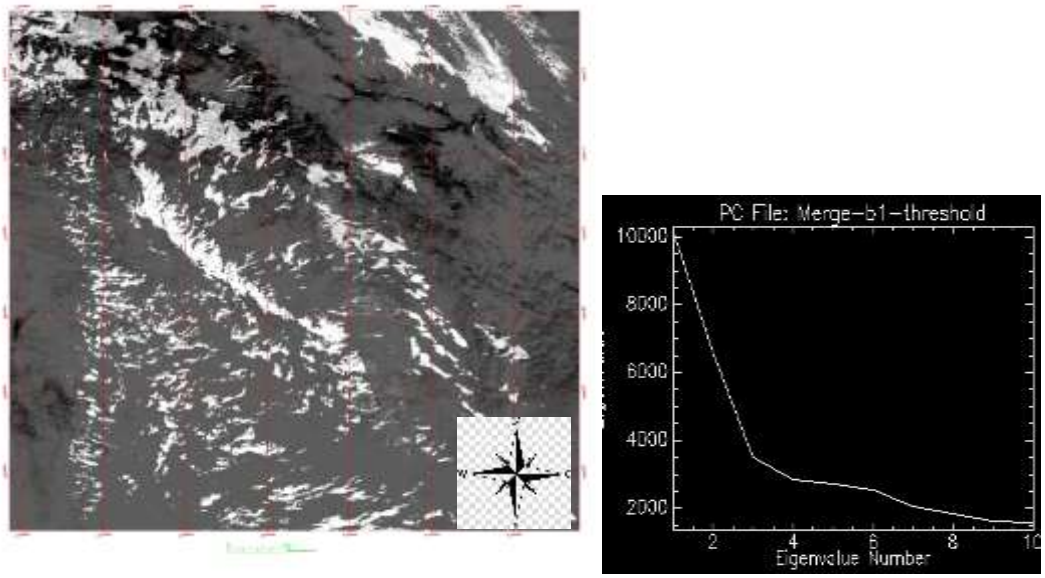

A, The Change of Bands 1

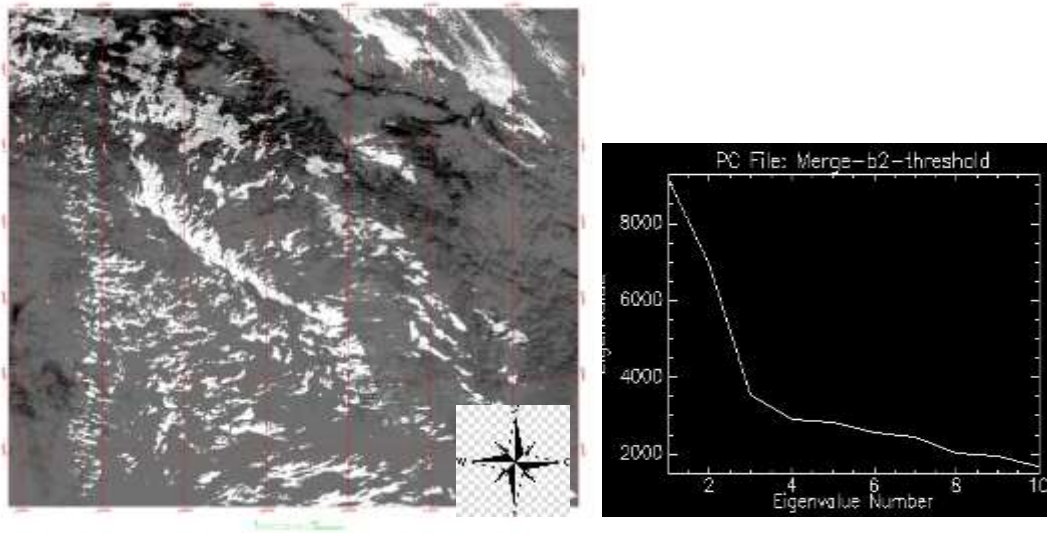

B, The Change of Bands

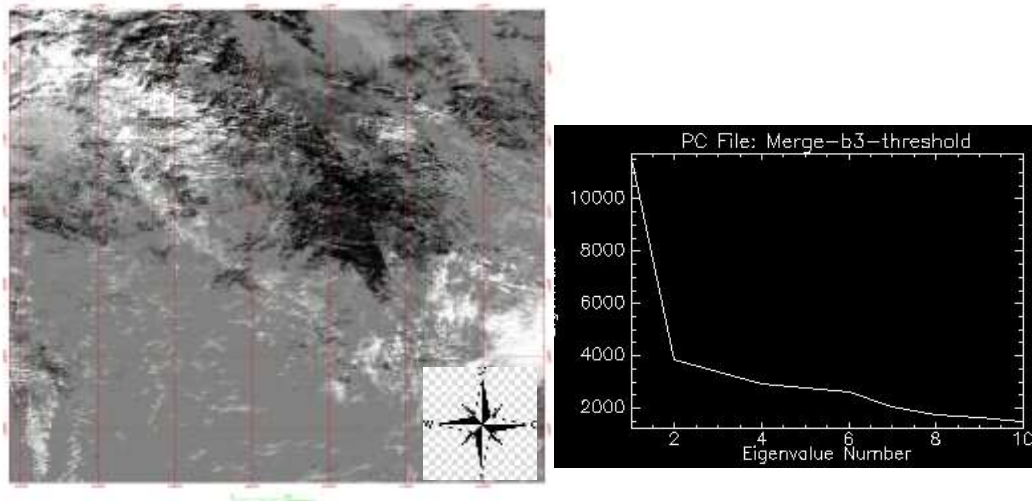

C, The Change of Bands 3

Figure 4: The Digital Change Detection Results of PCA kernel for Cloud Threshold Images

4.4 The Change Detection For Thermal Bands

For the surface temperature (band31 & band 32), also called emissivity bands, MOD11A1 mode of 1 km change detection was calculated using the PCA kernel. The wavelength of band 31 is (10.780-11.280) µm, and for band 32 is (11.770-12.270) µm. To overcome the wavelength of (10.78- 12.27) µm, the average of the bands was calculated, but the result does not represent the real data values. Therefore, since, the wavelengths of the two bands are continuous, the band 32 was used to extract the change due to long wavelength. .In general the clouds absorber all thermal energy, and hence appear cold in the thermal band, i.e. dark tone, [**11**]. The values of these thermal bands shows emissivity i.e. (0 to 1) unit less, as shown in Appendix A. The typical temperature to record bands 31 & 32 is 300 $\mathring{k}$. Thus, the user can calculate the radiated energy recorded by the sensor according to Stefan-Boltzmann law such as follows **;**

$$F = \in \sigma T^4 \quad (2)$$

Where,

F, is radiated energy per unit area recorder by sensor, watt/ m^2

$\in$, is the thermal emissivity, unitless.

σ, is Stefan-Boltzmann constant, 5.67×10^{-8} $W/m^2 \mathring{k}^4$

T, is temperature of thermal sources $\mathring{k}$.

For MODIS bands 31& 32, the F value is;

$$F = \in *459.27 \quad (3)$$

Hence, from the above discussion, the emissivity value can be use to extract the change of cloud for the 10 days period, see figure 5.

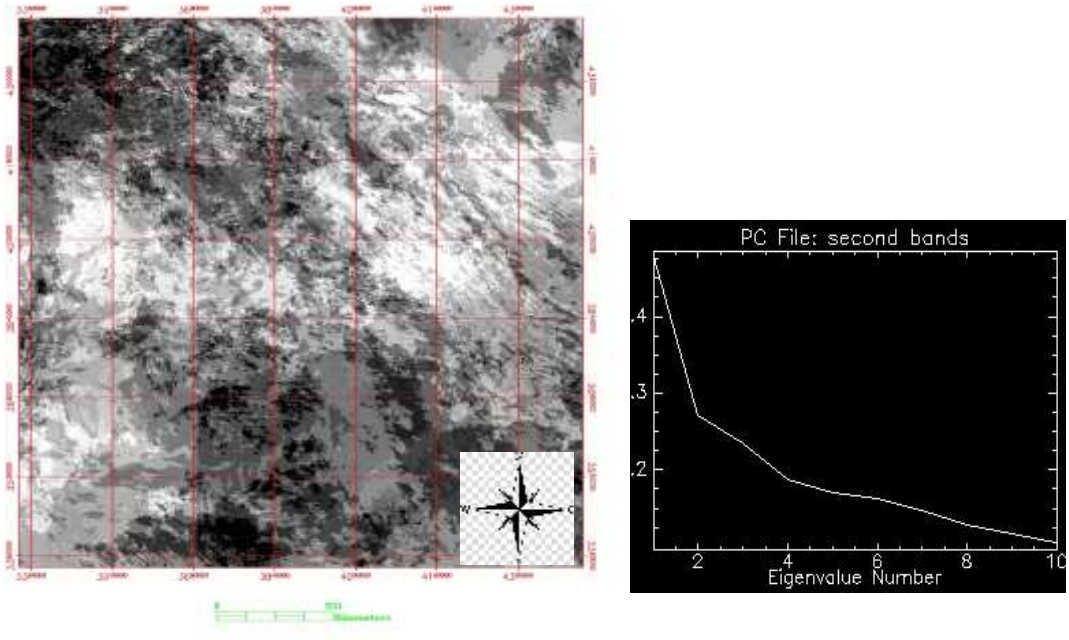

Figure 5: The Digital Change Detection Results of PCA kernel for Band 32, Emissivity

5. Results and Discussions

The results include the calculation of the cloud area on an image for each day of band 3 in the reflectance mode, as shown in Table 1. This paragraph was simply evaluated using the image statistics and the threshold values between (7000 to 10000), and above 10000.

Table 1: The Thin & Thick Cloud Area Calculation, Reflectance Mode, band 3

Date	Thin Cloud Area km^2	Thick Cloud Area km^2	Total Cloud Area km^2
12/14/2021	28679.5	782.25	29461.75
	6892	639.25	7531.25
12/16/2021	7962.75	1173.75	9136.5
	21781.75	5194.75	26976.5
12/18/2021	16392	8044	24436
	7767	8047.25	15814.25
12/20/2021	20045.5	8142.5	28188
	13680.75	9051.25	22732
12/22/2021	12928.75	4118.75	17047.5
	23795	8472.75	32267.75

From figure 4, A &B , the change of cloud areas are similar. This is a true case due to the high correlation between the NIR and Red bands, therefore, the clouds appear with high reflectance value in the visible band , i.e. band 3 (the Blue) is the best band for distinguishing the cloud, as shown in figure 4, C. Building on this fact the band 3 was selected to compute the clouds area for all days, as shown in Table 1. The thin clouds yielded a pixels values between (7000 to 10000), where, the thick clouds yielded a pixels values above 10000. These threshold values are corresponding to MODIS reflectance mode the images of spectral resolution between (8 to 16) bits. From the Table 1, it is clear that the clouds density was variable from day to day, where, the most cloudy day was 12/23/2021.

From the thermal emissivity band 32, it is observed that the clouds is cold, so the pixels value approach to zero. Distinguishing of clouds areas is based on the low pixel values. These calculations given in Table 2, in thermal band, the cloud density is difficult to estimate due to the low pixels values.

Table 2: The Cloud Area Calculation, Thermal Emissivity, band 32

Date	Total Cloud Area km^2
12/14/2021	910733
12/15/2021	275829
12/16/2021	520432
12/17/2021	743955
12/18/2021	362543
12/19/2021	379417
12/20/2021	421993
12/21/2021	369477
12/22/2021	404177
12/23/2021	848888

From Tables 1 and 2, the areas of cloud increase about 2.3 to 3 times at night over those of the daylight . This was realistic because in daylight, the Sun diffuses the clouds through thermal absorption and the clouds density becomes low. In fact, the values for these areas did not indicate perfect cloudy zones because the shaded areas in daylight appeared in zero

pixel values. Also, the table shows that the most cloudy day was 12/23/2012, as in the reflectance indication.

From Figures 4, C and 5, it is observed that the changes in clouds over the areas of the scenes occurred in absolutely different tones; i.e. bright tone for reflectance mode and dark tone for emittance mode. Many shifts in the clouds' positions can be noticed due to the difference in temperature between night and daylight. Using the ENVI image animation, it was found that the direction of wind for this cloudy case is from North-East to South-West. The 2-D scatter plots in Figure 4 A to C represent the Eigen values of the Forward PCA transform. These values start from the maximum value corresponding to PC1 to the minimum value for PC10. The overall integration of Eigen values is equal to1.

In the PCA change detection transform, some noise may appear in the images. This was due to the uncorrelated bands t used in the PCA kernel; i.e. the PCA kernel was applied for correlated data, such as the multi bands data from one scene, but the PCA change detectors dealt with the same band for different temporally scenes.

6. Conclusions

From the above results, the following can be concluded;

- The clouds can be detected and monitored from the multi band remotely data but with a suitable spatial resolution.
- The MODIS MOD09GA daily reflectance and MOD11A1 daily surface temperature were used to extract the results.
- The clouds appeared in high reflectance in the Blue band and low emittance in the thermal bands due to their absorption of all energy by the clouds.
- The digital change detection showed similar results between the NIR and Red bands, this is true due to the continuity of these bands.
- The change results showed that, the cloud areas vary from day to another, while, the most cloudy day was 12/23/2021.
- From the image animation, it was found that the direction of wind for the cloudy case is from North-East to South-West, whereas the daily weather records expected the wind direction to be East-Southeast.
- For a series of temporally data, the PCA change detector is convenient to extract the changes after files preparation.

References

[1] J. Huo, D. Lu, S. Duan, Y. Bi, and B. Liu, "Comparison of the cloud top heights retrieved from MODIS and AHI satellite data with ground-based Ka-band radar," *Atmospheric Measurement Techniques*, vol. 13, no. 1, pp. 1-11, 2020.

[2] Y. Jouybari Moghaddam and M. Aghamohamadnia, "A novel method for cloud detection in MODIS imagery," *ISPRS-International Archives of the Photogrammetry, Remote Sensing and Spatial Information Sciences*, pp. 221-224, 2013.

[3] E. Vermote, J. Roger, and J. Ray, "MODIS surface reflectance user's guide [R/OL]," *MODIS Land Surface Reflectance Science Computing Facility*, 2015.

[4] N. K. Ghazal, "Detection and interpretation of clouds types using visible and infrared satellite images," *Iraqi Journal of Physics*, vol. 15, no. 34, pp. 123-137, 2017.

[5] Z. Wan, " MODIS Land Surface Temperature Produce, Collection 6", University of California, 2013.

[6] A. K. M. Ali and F. K. M. Al Ramahi, "A study of the effect of urbanization on annual evaporation rates in Baghdad city using remote sensing," *Iraqi Journal of Science*, pp. 2142-2149, 2020.

[7] K. Strabala, "MODIS Sensor Characteristics", GEOSS/AMERICAS Remote Sensing Workshop São Paulo, Brazil 26, November, 2007.
[8] ENVI Tutorial, "Introduction to User Functions", www. spweather.com /enviuser /tutorial/programming_in_envi/User_Functions.
[9] F. K. Mashee and G. S. Hadi, "Study the wet region in Anbar province by use remote sensing (RS) and geographic information system (GIS) techniques," *Iraqi Journal of Science*, pp. 1333-1344, 2017.
[10] Y. Chen, Z. Ming, and M. Menenti, "Change detection algorithm for multi-temporal remote sensing images based on adaptive parameter estimation," *IEEE Access*, vol. 8, pp. 106083-106096, 2020.
[11] L. Sun, X. Mi, J. Wei, J. Wang, X. Tian, H. Yu, and P. Gan, "A cloud detection algorithm-generating method for remote sensing data at visible to short-wave infrared wavelengths," *ISPRS journal of photogrammetry and remote sensing*, vol. 124, pp. 70-88, 2017.

Appendix A
The MODIS Spectral Bands Characteristics, [7]

Band No.	Spectral Bands, nm	Usage	Notes
1	620 - 670	Land/Cloud/Aerosols Boundaries	Red, Reflectance
2	841- 876		NIR, Reflectance
3	459 - 479	Land/ Cloud/ Aerosols Properties	Blue, Reflectance
4	545 – 565		Green, Reflectance
5	1230 -1250		NIR, Reflectance
6	1628 - 1652		MIR, Reflectance
7	2105 - 2155		MIR, Reflectance
8	405-420	Ocean Color/ Phytoplankton/ Biogeochemistry	Short Blue, Reflectance
9	438 – 448		Blue, Reflectance
10	483 – 493		Blue, Reflectance
11	526 -536		Green, Reflectance
12	546 -556		Green, Reflectance
13	662 – 672		Red, Reflectance
14	673 -683		Red, Reflectance
15	743 -753		NIR, Reflectance
16	862 -877		NIR, Reflectance
17	890 -920	Atmospheric Water Vapor	NIR, Reflectance
18	931 -941		NIR, Reflectance
19	015 -965		NIR, Reflectance
20	3660 -3840	Surface Temperature	FIR, Emittance, 300 k
22	3929 - 3989		FIR, Emittance, 300 k
23	4021 - 4080		FIR, Emittance, 300 k̊
24	4433 -4498	Temperature Profile	FIR, Emittance, 250 k̊
25	4482 – 4549		FIR, Emittance, 275 k̊
27	6535 – 6895	Moisture Profile	FIR, Emittance, 240 k
28	7175 – 7475		FIR, Emittance, 250 k
29	8400 -8700		FIR, Emittance, 300 k
30	8580 - 9880	Ozone	FIR, Emittance, 250 k
31	10780 -11280	Surface Temperature	FIR, Emittance, 300 k̊
32	11770 -12270		FIR, Emittance, 300 k̊

33	**13185 -13485**	**Temperature Profile**	**FIR, Emittance, 260 $\mathring{k}$**
34	**13485 -13785**		**FIR, Emittance, 250 $\mathring{k}$**
35	**13785 -14085**		**FIR, Emittance, 240 $\mathring{k}$**
36	**14085 -14385**		**FIR, Emittance, 220 $\mathring{k}$**